

## Original Research Article

### Simulation of Meteorological Drought of Bankura District, West Bengal: Comparative Study between Exponential Smoothing and Machine Learning Procedures

#### Abstract

Simulation of drought is needed for proper planning and management of water resources. This study has been developed using the following five key points: a) primarily from rainfall Standard Precipitation Index (SPI), Percentage to Normal (PN), Decile based drought index (DI), Rainfall Anomaly Index (RAI), China Z Index (CZI), and Z-score are estimated on yearly basis (1901-2017), those indices are added and a new index standardized total drought ( $S_d$ ) has been established. b) Considering  $S_d$  as the input parameter a comparative assessment has been made between 4 individual models (3 models from exponential smoothing, 1 model from machine learning) in simulation and prediction of drought status of next 18 time steps (years) in Bankura District and Winexpo model outperforms the other models as it obtains minimized Standard Error (SE), Random Mean Square Error (RMSE), Mean Absolute Error (MAE), and Mean Absolute Percentage Error (MAPE) and highest Correlation coefficient ( $R^2$ ) value. c) The cumulative drought proneness of the region is also assessed and it is found that the whole district will be drought-prone within the year 2100. This region is historically a drought prone region and agricultural shock is the common issue. In such a circumstances simulation of drought is a good attempt. Though a lot of models already developed in case of simulation of drought but still a perfect, continuous long term prediction is a big issue to solve. Under such a circumstances, this study provides a comparative study between exponential smoothing and machine-learning procedures and also introduces a new combined index standardized total drought. Also the government should take the result seriously and should try seriously to mitigate the effects of drought.

**Keywords:** Simulation; meteorological drought; winexpo.

#### 1. Introduction

Drought is one of the natural disasters that human being has been suffering since the ancient era [1, 2, 3,4] and it is the costliest [5,6], long-lasting most severe natural hazard [7,8,9]. It is recurrent natural phenomena associated with the lack of water resources for a prolonged

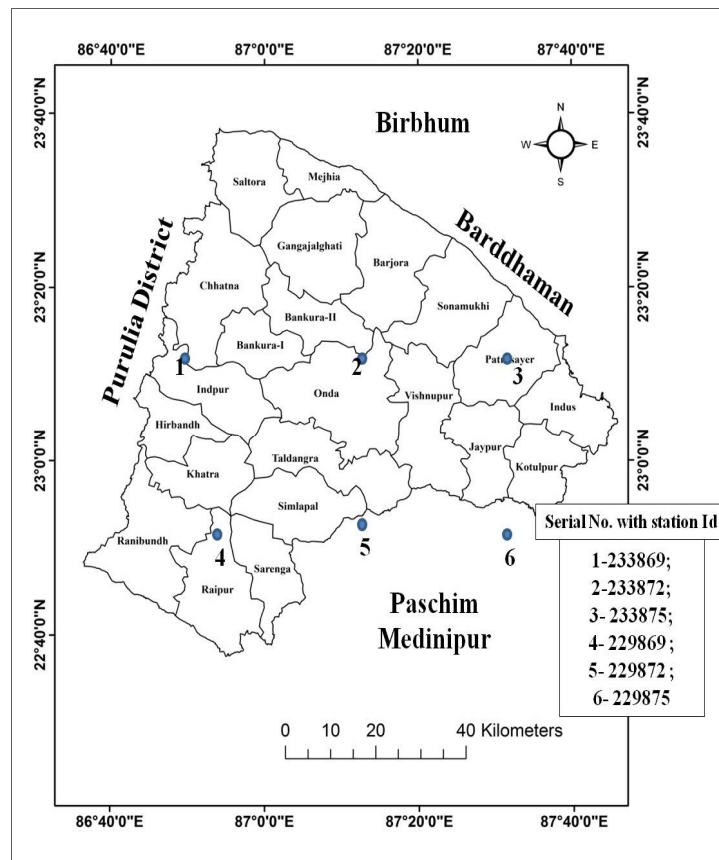
32 period of dryness[10,11,12] can occur in arid, semi-arid and rain-forested region [13,14]  
33 however confusion and debates among scholars prove that there are no universal accepted  
34 definitions of drought. Drought forecasting is a critical element in drought risk management  
35 [15]. Meteorological drought that transforms in a hydrological, agricultural and socio-  
36 economic events, onsets with a marked reduction in rainfall sufficient to trigger hydro-  
37 meteorological imbalance for a prolonged period [16,17,18,19]. Thus drought monitoring and  
38 assessment are hot topics among hydrologists and meteorologists and attract world-wide  
39 attention [18,19,20,21]; its' preparedness and mitigation depends upon the large scale drought  
40 monitoring and forecasting over a large geographical area [19,20,25]. Many drought  
41 forecasting models already develop in the field of civil engineering. Mishra and Desai (2006)  
42 [23] developed ARIMA and multiplicative seasonal ARIMA models to forecast drought  
43 using SPI series. These models are able to simulate drought up to 2 months lead time. Morid  
44 et.al 2007 [17] simulated Effective Drought Index (EDI) and SPI using Artificial Neural  
45 Network (ANN). They compared linear stochastic models with recursive multistep neural  
46 network model to the 6 months lead time. Barros and Bowden (2008) [25] employed self-  
47 organizing maps (SOM) and multivariate linear regression analysis to forecast SPI of Murray  
48 Darling basin of Australia in 12 months of forthcoming scenarios. Many scholars worldwide  
49 tested SVM in climatological and hydrological applications [26, 27]. There are several  
50 scholars used SVM to predict drought . Belayneh and Adamowski in 2012 [28] forecasted  
51 meteorological drought using neural network, wavelet neural network and SVM.  
52 Exponential smoothing is quite new in this field originally developed in the field of business  
53 mathematics in 1960. Exponential smoothing is able to simulate drought in a long term time  
54 frame. This study attempts to simulate drought using exponential smoothing in a long-term  
55 time frame.

## 56 **2. Study Area and Background Information**

57 The District Bankura is bounded by 22°38' N to 23°38' N and longitude 86°36' E to 87°47'E  
58 covering an area of 6,882 square Kilometers (2,657sq. mile). River Damodar creates the  
59 north and north-east boundary of the district [29, 30, 31]. The neighboring districts are  
60 Bardhaman in the north, Paschim Medinapore in the south, Hoogly in the east and Purulia in  
61 the west (Figure 1). Bankura is a historically a drought prone district and if no supportive  
62 action taken quickly in this regard the condition will get much severe in the upcoming  
63 periods [32,33,34,35].

64

65  
66  
67  
68  
69  
70  
71  
72  
73  
74  
75  
76  
77  
78  
79



80 **Figure 1** Bankura Location Map and location of Meteorological Stations

81 Bankura is located in the south western central part of the State of West Bengal belonging  
82 transition zone between the plains of Bengal on the east and Chhota Nagpur plateau on the  
83 West [34, 35]. It is a part of Midnapur Division of the State and a part of “Rarh” region thus  
84 can be stated as “Rarh in Bengal” [31, 32]. The areas to the east and north-east are rather flat  
85 belonging to the low lying alluvial plains, known as rice bowl of Bengal [33,34,35].

### 86 3. Material and Method

87 Figure 2 constructively describes the methodological overview of this paper. Monthly rainfall  
88 data 1901-2017 has been used for overall analysis and 1901 to 1978 data obtained from Govt.  
89 of India water portal website. From 1979 to 2014 daily station wise rainfall data obtained  
90 from National Centres for Environmental Protection (NCEP) official website. The rainfall  
91 data were collected from Disaster Management Plan of Bankura District 2017 published by  
92 District Disaster Management Cell (Table 1) and got 6 individual rainfall stations available

93 for Bankura District and monthly and daily rainfall data have been added to get yearly  
 94 rainfall trend. Thus 117 years are taken into consideration.

95 **Table 1** Station list according to the NCEP data set

<b>Id of Stations associated Bankura</b>	<b>Longitude</b>	<b>Latitude</b>	<b>Elevation(m)</b>
229869	86.875	22.9488	133
229872	87.1875	22.9488	61
229875	87.5	22.9488	34
233869	86.875	23.261	127
233872	87.1875	23.261	95
233875	87.5	23.261	46

96

97

98

99

100

101

102

103

104

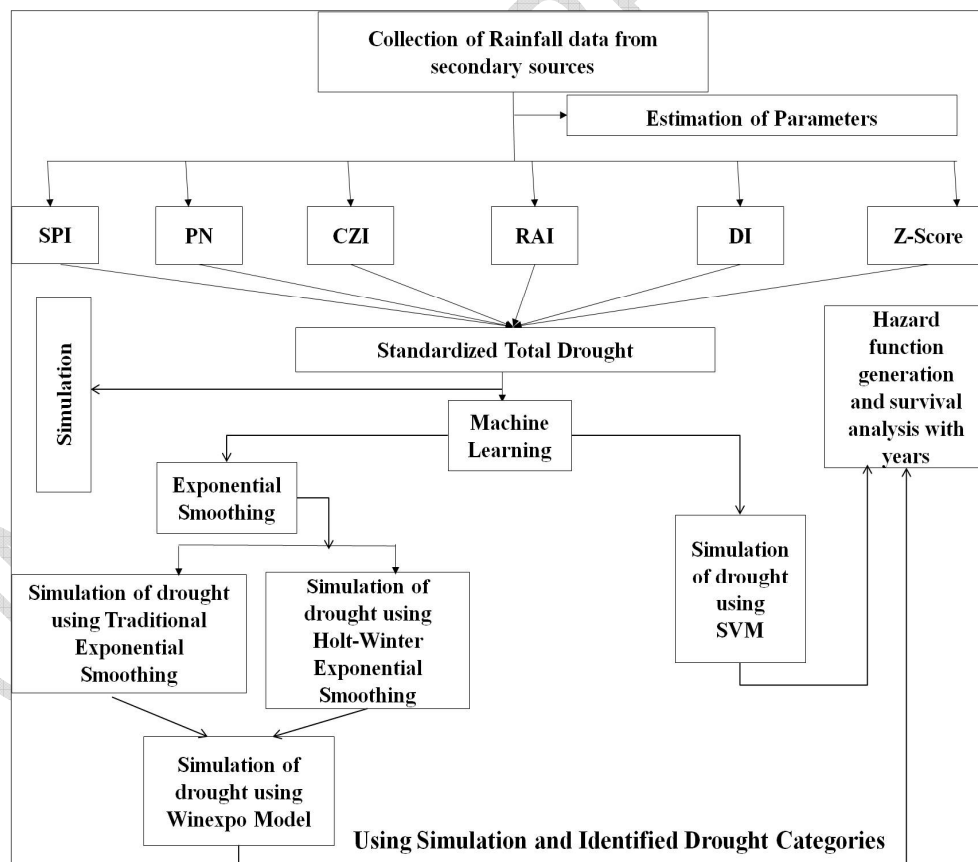
105

106

107

108

109



110

**Figure 2** Methodological Overview

111

112

113

114

115

116

117

118

119

120

### 121 **3.1 Formation of Standardized Total Drought ( $S_d$ )**

122 There are several indices developed to assess meteorological drought but the most common  
 123 are SPI [37,38], DI [39,40], PN [5], Z-Score [5], RAI [41,42] and CZI [43]. First of all, from  
 124 the rainfall data, the above mentioned 6 well-known indices i.e. SPI, DI, CZI, PN, Z-score,  
 125 and RAI have been estimated on yearly basis and later those are combined and formed a new  
 126 Index Standardized Total Drought ( $S_d$ ). So, those six indices are utilized to estimate the true  
 127 nature of meteorological drought and standardized total drought (yearly basis) becomes the  
 128 sole input variable for every models of our study.

129 It can be computed as follows:

$$130 \text{ Total Drought}(T_d) = (\text{SPI} + \text{DI} + \text{PN} + \text{ZScore} + \text{RAI} + \text{CZI}) \quad (1)$$

$$131 \text{ Standardized Total Drought}(S_d) = \frac{T_d - \overline{T_d}}{\delta} \quad (2)$$

132 Where,  $T_d$  is the total drought.

133  $\overline{T_d}$  is the mean of  $T_d$

134  $\delta$  is the standard deviation of the total drought.

135 Based on estimated  $S_d$  values the individual drought categories are subdivided into 9 sub-  
 136 groups. he whole subgroups are ranging between  $<-10$  to  $>10$  category and  $<-10$  denotes the

137 most extreme category whereas >10 denotes wet category. Every 9 sub categories are coded  
 138 as 1 to 9 (table 2).

139 **Table 3 Probable classes of Standardized Total Drought ( $S_d$ )**

Categories of Drought	Code	Ranges of Drought
Most Extreme	1	<-10.00
Extreme	2	-3.00 to -10.00
Severe	3	-2.99 to -2.50
Severe Moderate	4	-2.49 to -2.35
Moderate	5	-2.35 to -1.15
mild drought	6	-1.15 to 1
Normal	7	1-5
Extreme Normal	8	5-10
Wet	9	>10

140

### 141 **3.2 Exponential and Holt-Winter Forecast and Winexpo Method:**

142 Exponential smoothing is the technique to smoothing the time series in exponential window  
 143 function. Exponential smoothing assigns decreasing weights over time. Holt in 1957 and  
 144 Winter in 1960 developed smoothing technique and later their method was combined and  
 145 making Holt-Winter smoothing technique to forecast the recursive trend from the historically  
 146 observed data series [44]. Here we use the single exponential smoothing technique as Kaleker  
 147 in 2004 [45] used in his thesis:

$$148 \quad S_{t+1} = \alpha * y_t + (1 - \alpha) * S_t \quad 0 < \alpha < 1, t > 0 \quad (3)$$

149 Eq. (11) can be written as

$$150 \quad S_{t+1} - S_t = \alpha * \epsilon_t \quad (4)$$

151 The Holt-Winter method time series can be represented using the following model:

$$152 \quad y_t = (b_1 + b_2 t) * S_t + \epsilon_t \quad (5)$$

153 Where  $b_1$  is the permanent component,  $b_2$  is the linear trend component,  $S_t$  is the  
 154 multiplicative seasonal factor,  $\epsilon_t$  is the random error component,  $t$  is the time and  $t+1$  is the  
 155 lead time from  $t$ .

156 From the Eq. (13)

$$157 \quad S_t = \frac{y_t}{b_1 + b_2 t} + \epsilon_t \quad (6)$$

158 Sum of all the seasons can be written as

$$159 \quad \sum_{t=1}^{12} S_t = M \quad (7)$$

160 Where L is the length of the year.

161 So, the Eq. (7) can be written as,

$$162 \quad \sum_{t=1}^{12} y_t = (b_1 + b_2 \sum_{t=1}^{12} t) * \sum_{t=1}^{12} S_t + \epsilon_t \quad (8)$$

163 Assuming,  $\sum_{t=1}^{12} y_t = Y$ ,  $\sum_{t=1}^{12} t = T$  and  $\sum_{t=1}^{12} S_t = M$  we get from Eq. (16)

$$164 \quad Y_t = (b_1 + b_2 T) * M + \epsilon_t \quad (9)$$

165 And Eq. (14) can be written after the sum of all the seasons

$$166 \quad M = \frac{Y_t - \epsilon_t}{b_1 + b_2 T} \quad (10)$$

167 Winexpo method has been developed by us to combine the traditional exponential and Holt-

168 Winter method. Combining Eq. (12) and Eq. (18) we get,

$$169 \quad \frac{S_{t+1} - S_t}{M} = \frac{\alpha \epsilon_t}{\frac{Y_t - \epsilon_t}{b_1 + b_2 T}} \quad (11)$$

$$170 \quad \text{Or, } \frac{S_{t+1} - S_t}{M} = \frac{\alpha * (b_1 + b_2 T)}{(Y_t - \epsilon_t)} + \epsilon_t \quad (12)$$

171 Winexpo is one of the integrative models as it holds the combination of Holt-Winter  
172 exponential smoothing and traditional exponential smoothing.

173

174

### 175 **3.4 Support Vector Machine model (SVM)**

176 Support Vector Machine (SVM) is the supervised learning models that analyse data used for  
177 classification and regression analysis [44, 45, 46, 47, 48,49]. The x related all points can be

178 mapped in the hyperplane can be defined by the relation  $\sum_i \alpha_i k(x_i, x) = \text{constant}$  where  $k(x_i,$

179  $x)$  is the kernel function used to suit the problem. Kernel function becomes small where  $y$

180 grows further away from  $x$  so it becomes the matter of closeness of each point of  $y$  to  $x$ . With

181 the kernel function SVM actually use the relative closeness between the each point in the  
182 feature space. The detailed method of analysis can be expressed as following:

183 Suppose our training data is consist of N pairs  $(X_1, Y_1), (X_2, Y_2), \dots, (X_n, Y_n)$ ; where  
184  $X_i \in \mathbb{R}^p$  and  $Y_i \in \{-1, 1\}$ . Define a hyperplane by,  $\{x: f(x) = x^T \beta + \beta_0 = 0\}$ , where  $\beta$  is a unit  
185 vector. A classification rule induced by  $f(x)$  is  $G(x) = \text{sign} \{x^T \beta + \beta_0\}$ . Now the signed  
186 distance from the point  $x$  to the hyperplane is 0. Here we are able to find the hyperplane that  
187 creates biggest margin between training points for class 1 and -1. So, the optimization  
188 problem just reverses and forms the following dimension:

$$189 \max_{\beta, \beta_0, \|\beta\|=1} = M \quad (13)$$

190 Subject to,

$$191 \text{subject to, } y_i \{x^T \beta + \beta_0\} \geq M \quad ; \quad i = 1, 2, \dots, N \quad (14)$$

192 We have used here Least Square Support Vector Machine is based on structural risk  
193 minimisation in the model weight. It counters convex quadratic programming associated with  
194 Support Vector Machine (SVM) .The least square version of the SVM classifier is obtained  
195 by reformulating the minimization problem as

$$196 \min J_2(w, b, e) = \frac{\mu}{2} x^T \beta + \frac{\infty}{2} \sum_{i=1}^N e_i^2$$

197 Subject to equality constraints,

$$198 y_i [x^T \beta + \beta_0] = 1 - e_i, \quad i=1, 2, \dots, n \quad (15)$$

199 Eq. 36 can be written as

$$200 e_i = 1 - y_i [x^T \beta + \beta_0] \quad (16)$$

201 The eq. 37 hold the case of regression. To solve the eq. 37 we use Lagrangian multiplier by  
202 which it can be solved.

$$203 L_2(w, \beta, e, \alpha) = J_2(w, e) - \sum_{i=1}^n \alpha_i \{[\beta + \beta_0] + e_i - y_i\} \quad (17)$$

204 Where,  $\alpha_i \in \mathbb{R}$ , the Lagrangian multipliers. For evaluation performance test of SVM we use  
205 the error estimation and Kappa Coefficient statistic as well as the accuracy. The definition of  
206 Cohen's Kappa is as follows:

$$207 k = \frac{p_0 - p_e}{1 - p_e} \quad (18)$$



208 Where,  $P_0$  is the relative observed agreement among variables;  $P_e$  is the hypothetical  
 209 probability of chance agreement. If the rates are in the complete agreement then  $k = 1$  and if  
 210 there is no agreement then  $k = 0$ .

### 211 3.7 Estimation of Cumulative Hazard Proneness

212 To estimate the cumulative drought-proneness of the study region over the years we took help  
 213 of the hazard function and survival analysis. Let  $T$  be a non-negative random variable  
 214 representing the waiting time until the occurrence of an event. For simplicity we can adopt  
 215 the term 'survival analysis' referring to the event of interest as 'hazard proneness' and to the  
 216 waiting time we state as 'survival time'. We can assume  $T$  is a continuous random variable  
 217 with probability density function (p.d.f.)  $f(t)$  and cumulative distribution function (c.d.f.)  
 218  $\Pr\{k < t\}$  given that probability that the event has occurred by duration  $t$ . Complement of  
 219 c.d.f. the survival function becomes

$$220 S(t) = \Pr\{T \geq t\} = 1 - F(t) = \int_t^{\infty} f(x) dx \quad (19)$$

221 Which gives probability of being 'less drought prone' just before duration  $t$  more generally  
 222 the probability that the event of interest has not occurred by duration  $t$ . Here we use the  
 223 following distribution of  $T$  is given by hazard function or instantaneous route of occurrence  
 224 of the event defined as

$$225 \Omega(t) = \lim_{dt \rightarrow 0} \frac{\Pr\{t \leq T < t+dt, T \geq t\}}{dt} = \frac{f(t)}{S(t)} \quad (20)$$

226 Where  $f(t)$  is the derivative of  $S(t)$

$$227 S_t = \exp\left\{-\int_0^t \Omega(x) dx\right\} \quad (21)$$

228

229

### 230 3.8 Error Estimation

#### 231 3.8.1 Standard Error (SE)

232 The standard error can be stated as [50, 51]

$$233 SE = \frac{\partial}{\sqrt{n}} \quad (22)$$

234 Where  $\partial$  the standard deviation of the distribution and  $n$  is the number of samples.

### 235 3.8.2 Root of Mean Squared Error (RMSE)

236 Root of mean squared deviation can be stated as

$$237 \text{ RMSE} = \frac{\sqrt{\sum_{t=1}^T (\bar{y}_t - y_t)^2}}{\sqrt{T}} \quad (23)$$

238 Where, The RMSD of predicted values for  $\bar{y}_t$  times t of a regression's dependent  
239 variable  $y_t$  with variables observed over T times.

### 240 3.8.3. Mean Absolute Error (MAE)

241 MAE measures average magnitude errors in the set of predictions without considering their  
242 direction. It is the average over the test sample of the absolute differences between prediction  
243 and actual observation where all individual differences have equal weight:

$$244 \text{ MAE} = 1/n \sum_{j=1}^n |y_j - \bar{y}_j| \quad (24)$$

245 Where  $y_j$  is the observed value and  $\bar{y}_j$  is the predicted value.

### 246 3.9.4. Mean Absolute Percentage Error (MAPE)

247 Mean Absolute Percentage Error (MAPE) is a measure of prediction accuracy of a  
248 forecasting method of accuracy. MAPE can be stated as

$$249 \text{ MAPE} = \frac{100\%}{n} \sum_{t=1}^n \left| \frac{y_t - F_t}{y_t} \right| \quad (25)$$

250 Where,  $y_t$  is the actual value and  $F_t$  is the forecasted value.

251

252

253

## 254 3.10 Significance test

### 255 3.10.1 Anderson-Darling Test

256 The Anderson-Darling test is the hypothesized distribution is F, and cumulative distribution  
257 is  $F_n$  and the formula can be written as

$$258 A^2 = n \int_{-\infty}^{\infty} \frac{(F_n(x) - F(x))^2}{F(x)(1 - F(x))} dF(x) \quad (26)$$

### 259 3.10.2 Kolmogorov-Smirnov Test

260 Kolmogorov Smirnov test is a nonparametric test of the equality of continuous one  
261 dimensional probability distribution with compare of a sample with reference probability  
262 distribution [53,54]. Kolmogorov Smirnov test statistic can be expressed as

$$263 F_n(x) = 1/n \sum_{i=1}^n I_{[-\infty, x]}(X_i) \quad (27)$$

264 Where  $I_{[-\infty, x]}(X_i)$  is the indicator function, equal 1 if  $(X_i) \leq x$  and equal to 0 otherwise.

265 The Kolmogorov-Smirnov statistic of a given cumulative function  $F(x)$  is

$$266 D_n = \sup_x (F_n(x) - F_x) \quad (28)$$

267 Where sup is the supremum of the set of distance between the  $F_n(x)$  and  $F_x$ . In our case this  
268 model has been run at 95% significance level.

### 269 3.10.3 Shapiro -Wilk Test

270 Shapiro and Wilk test of the normality formula can be written as,

$$271 W = \frac{(\sum_{i=1}^n a_i x_i)^2}{\sum_{i=1}^n (x_i - \bar{x})^2} \quad (29)$$

272  $a_i$  is the  $(a_1, \dots, a_n)$ ,  $\bar{x}$  is the mean.

273 The constants  $a_i$  can be written as  $(a_1, \dots, a_n) = \frac{m^T V^{-1}}{(m^T V^{-1} V^{-1} m)^{1/2}}$  here

$$274 m = (m_1, \dots, m_n)^T$$

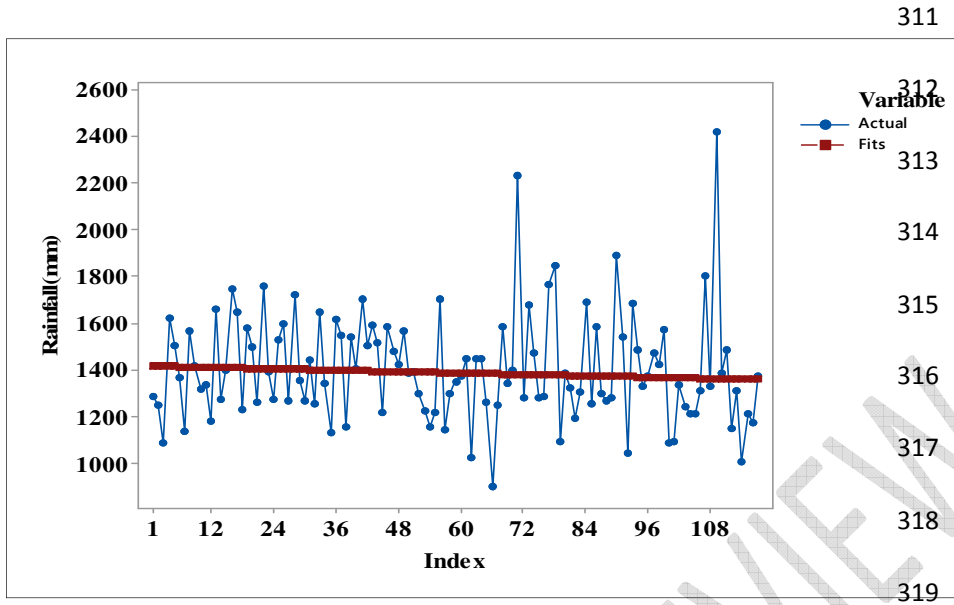
275 and  $m_1, \dots, m_n$  are the expected values of the order statistics of independent and  
276 identically distributed random variables sampled from the standard normal distribution,  
277 and  $V$  is the covariance matrix of those order statistics.

278

## 279 4. Results and Discussion

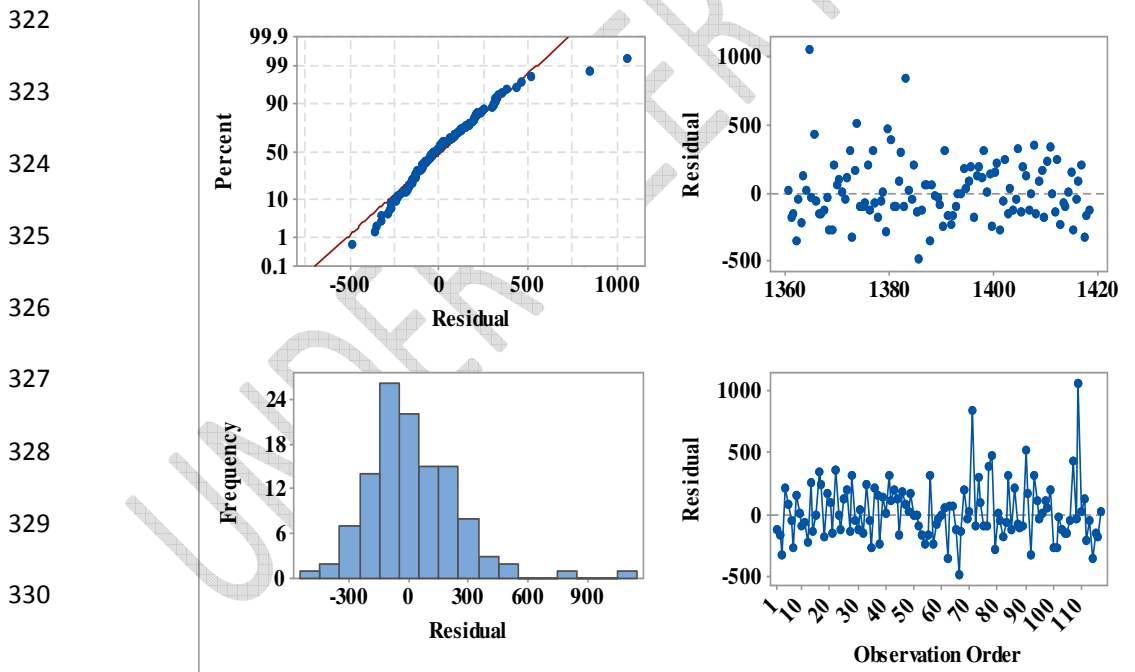
280 Fluctuation of rainfall and a negative exponential trend are specified in Figure 3 ( $Y_t =$   
281  $1418.88 \times (0.999642)^t$ ). Rainfalls are more or less normally distributed at 95% confidence  
282 interval (Figure 4a). Residuals versus fit plot (Figure 4b) displays that the points are  
283 randomly distributed on both sides of zero with no recognisable patterns thus our rainfall data  
284 are having a constant variance. Residuals of rainfall are having a mean close to zero and the

285 histogram is symmetric close to around zero (Figure 4c). Residuals versus order fit (Figure  
286 4d) shows that the residuals fall randomly around the centre line. Before proceed with rainfall  
287 and estimated 6 indices the reliability of those 6 indices are judged using Cronbach's Alpha.  
288 The overall value of Cronbach's alpha is 0.9694. Average SPI and Z-score between the time  
289 frame 1901-1939 are -0.06 and 0.299 , in between 1940 -1980, 0.037 and 0.382 respectively  
290 and from 1980-2035 the average SPI and Z-score becomes -2.345. Average PN value from  
291 1901-1939 is 100.792 %, 1940-1980 PN becomes 100.641%; 1980-2035 it is diminished and  
292 become 98.967%. In the same way average DI is estimated and from 1901-1939 DI 5.76%,  
293 1940 to 1980 5.73% and DI from 1980 to 2035 4.64% value of DI is obtained. CZI and RAI  
294 are also decreased from 0.32 (1901-1939) and 0.38 to 0.26 (1940-1980) ,0.28 and later 1980-  
295 2035 it reaches to 0.14 and 0.19. Overall all the indices attain negative trend. SPI, PN, DI,  
296 RAI, CZI and Z-score are added and a new index Standardized Total Drought ( $S_d$ ) has been  
297 formed to estimate overall trend of meteorological drought of Bankura District. Estimation  
298 and prediction of the trend of  $S_d$  using the traditional exponential smoothing has been done  
299 and a slightly negative trend is obtained (Values reach to -0.143 in 2035) (Figure 5a). The  
300 residuals of traditional exponential smoothing trend values are ranging between -15 to +5  
301 (Figure 5b). In case of traditional exponential smoothing the average value between 1901-  
302 1939 experiences -0.170, 1940 to 1980 the value reaches to -0.034 whereas between the 1980  
303 to 2035 the average value attains -0.134 thus overall trend is seemed to be more drought  
304 prone in recent upcoming periods. Similarly using Holt-Winter exponential smoothing  
305 analysis and prediction of drought has been done (Figure 5c) and residuals are fitted  
306 randomly as histogram plot based on the centre line (ranging between -2 to +5 range) (Figure  
307 5d). In case of Holt-Winter exponential smoothing the average value between 1901-1939  
308 achieve -0.163, between the time frame 1940-1980 and 1980 to 1935 it attain 0.061 and -  
309 0.261 values respectively. The combined model Winexpo attains 0.423 for 1901-1939, 0.51  
310 for 1940-1980 and -1.423 for 1980-2035.

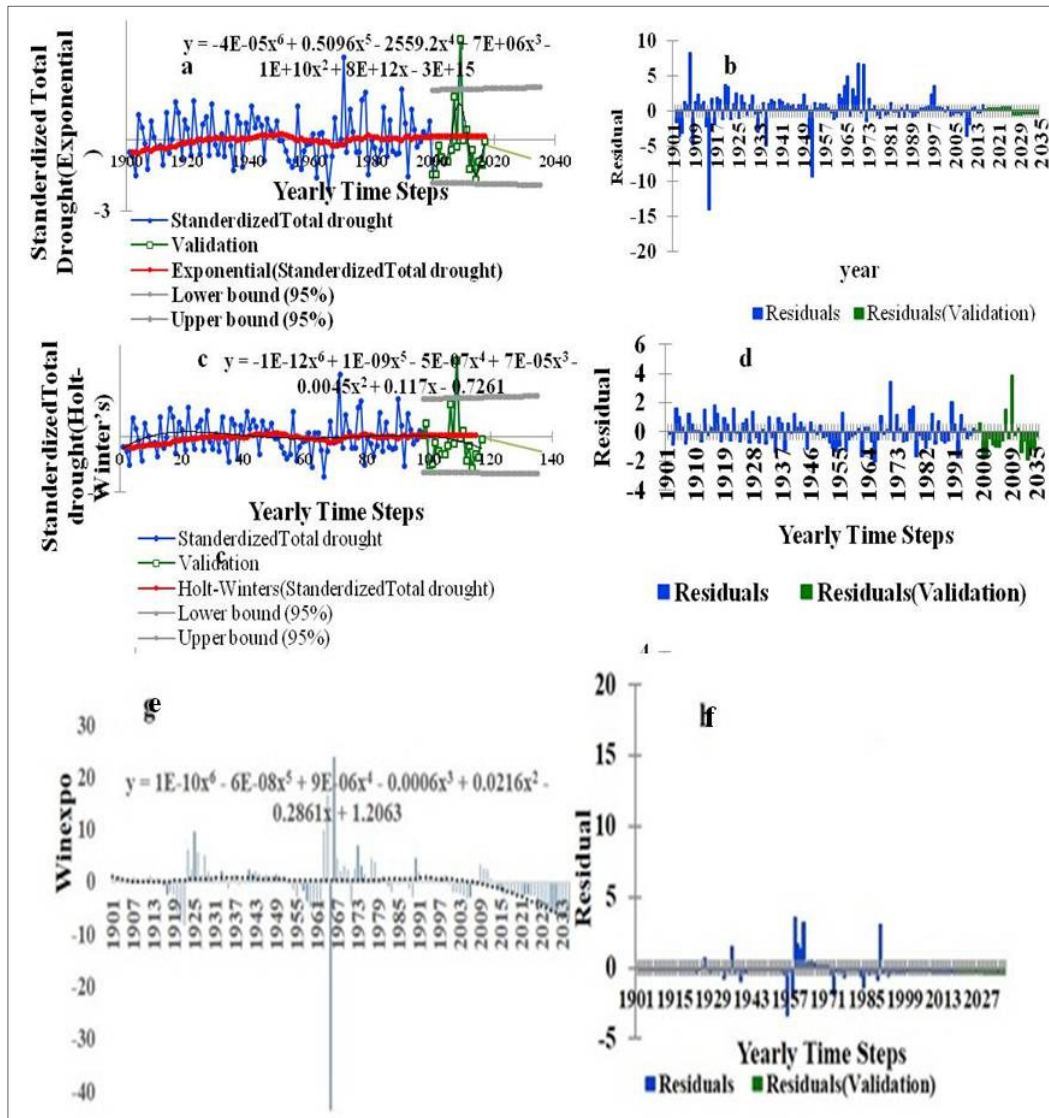


319  
320 **Figure 3** All station accumulated rainfall according to yearly time steps (1901-2017)

321



322  
323  
324  
325  
326  
327  
328  
329  
330  
331 **Figure 4a** Normal probability Plot of Rainfall **Figure 4b** Fitted value of rainfall vs. Residual  
332 value **Figure 4c** Residual value versus Frequency value **Figure 4d** Observation order vs.  
333 Residual value



334 **Figure 5** Exponential Smoothing models and associated Residual Plots a) Exponential  
 335 Smoothing c) Holt-Winter Smoothing e) Winexpo Simulation

336 From the true classes determined from the categories of  $S_d$  SVM is capable to predict the  
 337 nature of drought category. A user friendly SVM tool LSSVM is used to implement the  
 338 classification of drought status of Bankura District. At data pre-processing stage raw values  
 339 of  $S_d$  are linearly rescaled into  $[-1, 1]$  using the ranges of their minimums and maximums for  
 340 binary distribution of classifiers. Applying the SVM each category against all is estimated in  
 341 every case. In case of Extreme vs. others the model is obtained 43 support vectors, for  
 342 extreme normal the model is obtained 33 support vectors, for mild drought the model obtains  
 343 34 support vectors, most extreme the model obtains 28 support vectors, normal vs. others  
 344 obtains 51 support vectors, severe vs. others obtains 8 support vectors and wet vs. others

345 obtains 20 support vectors. From the observed true classes of 135 observations (used  
 346 simulated value using Winexpo) drought probability classes are predicted by SVM. SVM  
 347 performs with a medium accuracy level. According to SVM identified drought categories  
 348 over years over 80% years are concentrated within severe moderate, severe, extreme and  
 349 most extreme categories and about 20% years are concentrated within Moderate, Normal, and  
 350 Extreme Normal, wet categories (Figure 6a) whereas according to Winexpo identified  
 351 drought categories 36% years are mingled with severe moderate, severe, extreme, most  
 352 extreme and moderate categories and over 64% are mingled with normal, mild, extreme  
 353 normal and wet categories (Figure 6b). The extreme normal versus others, wet versus others,  
 354 mild versus others, normal versus others training sample sets achieve over 90% accuracy  
 355 whereas extreme and most extreme versus others and severe moderate versus others category  
 356 training samples achieve less than 30% accuracy (Table 4). Overall average SVM achieve  
 357 0.724 as Cohen's Kappa and overall 60% accuracy has been achieved. So, SVM has  
 358 performed moderately well in prediction of drought of our study area.

359

360

361

362

363

364

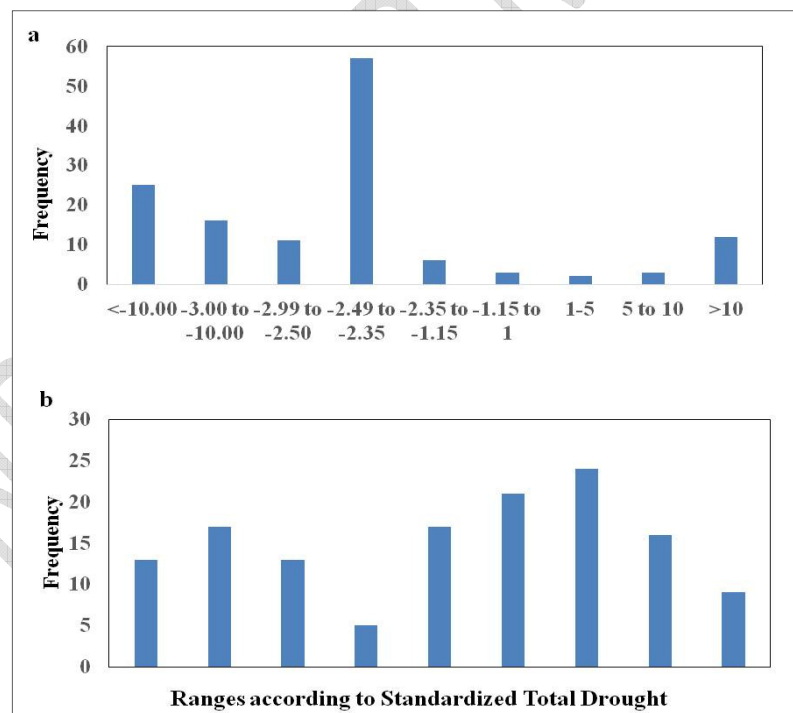
365

366

367

368

369



370 **Figure 6** Frequency of drought under each drought categories a) based on simulation model  
 371 of SVM b) based on simulation of Winexpo

372

373 **Table 4 Performance matrix of Support Vector Machine (SVM)**

<b>Training set</b>	<b>Accuracy</b>	<b>Cohen's kappa</b>
<b>Extreme versus Others</b>	0.847	0.978
<b>Extreme Normal versus Others</b>	0.187	0.086
<b>Moderate versus Others</b>	0.987	0.987
<b>Most Extreme versus Others</b>	0.847	0.978
<b>Normal versus Others</b>	0.253	0.222
<b>Severe versus Others</b>	0.987	0.998
<b>Severe Moderate versus Others</b>	0.876	0.965
<b>Wet versus Others</b>	0.153	0.042
<b>Mild versus Others</b>	0.165	0.078

374

375 The significance test using three individual tests has been run at 95% and 99%  
376 confidence interval (Table 5). The traditional exponential smoothing experiences probability  
377 value 0.004 for Anderson-Darling test, 0.005 for Shapiro-Wilk test and 0.004 by  
378 Kolmogorov-Smirnov test. The Holt-Winter exponential smoothing attains 0.003  
379 probabilities for Anderson-Darling test, 0.004 for Shapiro-Wilk test and 0.001 for  
380 Kolmogorov-Smirnov test. Winexpo model also attains probability value 0.002 for Anderson-  
381 Darling test, 0.004 for Shapiro-Wilk test and 0.003 for Kolmogorov-Smirnov test. The  
382 Bayesian model of LSSVM extreme category vs. other categories experiences 10.275 as  
383 Anderson-Darling test statistic value, 0.527 as Shapiro-Wilk test statistic value and 0.435 as  
384 KS test statistic value. LSSVM Bayesian most extreme vs. other category is mingled with  
385 5.543 as Anderson-Darling test statistic, 0.727 as Shapiro-Wilk test statistic and 0.316 as KS  
386 test statistic. SVM extreme normal vs. other categories achieves 2.165 as Anderson-Darling  
387 test statistic, 0.904 as Shapiro-Wilk test statistic and 0.482 as KS test statistic value.  
388 Similarly, Mild versus others, severe versus others, severe moderate versus others and wet  
389 versus others are also calculated (Table 5). All the Anderson–Darling test is successful and  
390 valid at 95% confidence interval as the significance level P-value achieves <0.005 value in all



391 the nine combinations. Shapiro-Wilk and KS test for all the SVM nine possible combinations  
 392 the probability value is <0.010 that means those values are significant at 99% confidence  
 393 interval. Overall SVM model is significant at 95% confidence interval (in case of Anderson-  
 394 Darling test) and 99% significance level (in case of Shapiro-Wilk test and KS test). As P  
 395 values are <0.005 and <0.010 for all the cases the distribution is not normal here and null  
 396 hypothesis that there were no difference between the observed class and predicted class can  
 397 be rejected and the alternative hypothesis is accepted. The error estimation and goodness of  
 398 fit statistics (Table 6) of the individual models indicate that Winexpo attains the lowest error  
 399 and highest R-square value in comparison with the other models altogether.

400 **Table 5 Error Estimation and Goodness of fit statistics (for error estimation 0.001 used**  
 401 **as a multiplicative factor)**

Model Name	SE	Adjusted RMSE	Adjusted MAE	Adjusted MAPE	R <sup>2</sup> (using Linear kernel)
<b>Traditional exponential smoothing</b>	0.024	0.996	0.790	25.65	0.39
<b>Holt-Winter Smoothing</b>	0.026	1.006	0.654	95.43	0.04
<b>Winexpo Model</b>	0.111	1.64	0.445	49.53	0.35
<b>SVM-Most Extreme versus others</b>	3.080	0.049	0.045	4.559	0.99
<b>SVM-Extreme versus others</b>	1.303	0.038	0.019	2.048	0.94
<b>SVM-Severe versus others</b>	11.180	0.026	0.026	1.915	0.95
<b>SVM-Severe moderate versus others</b>	11.345	0.023	0.045	1.934	0.99
<b>SVM-Moderate versus others</b>	5.533	0.015	0.008	0.833	0.99
<b>SVM-Mild versus others</b>	5.333	0.020	0.013	1.413	0.97
<b>SVM-Normal versus others</b>	1.668	0.033	0.019	2.048	0.52
<b>SVM-Extreme Normal versus others</b>	7.580	0.018	0.014	1.487	0.35

<b>SVM-Wet versus others</b>	83.724	0.001	0.008	0.900	0.34
<b>Overall SVM versus other</b>	0.130	0.02175	0.022	1.904	0.78

402

403 **Table 6** Significance test of the models

<b>Standardized Total Drought</b>	<b>Anderson-Darling Test</b>		<b>Shapiro-Wilk Test</b>		<b>Kolmogorov-Smirnov Test</b>		<b>Type of Model</b>
	<b>Test Statistic</b>	<b>Significance Level</b>	<b>Test Statistic</b>	<b>Significance Level</b>	<b>Test Statistic</b>	<b>Significance Level</b>	
<b>Traditional Exponential Smoothing</b>	8.827	0.004 (<0.005)	0.916	0.005 (<0.05)	0.169	0.004 (<0.005)	Exponential Smoothing
<b>Holt-Winter Exponential Smoothing</b>	7.192	0.003 (<0.005)	0.917	0.004 (<0.005)	0.163	0.001 (<0.005)	
<b>Winexpo Model</b>	28.790	0.002 (<0.005)	0.529	0.004 (<0.005)	0.363	0.002 (<0.005)	
<b>SVM-Extreme versus others</b>	10.275	<0.005	0.527	<0.010	0.435	<0.010	Machine Learning
<b>SVM-Extreme normal versus others</b>	2.165	<0.005	0.904	<0.010	0.482	<0.010	
<b>SVM-Mild vs. others</b>	11.598	<0.005	0.482	<0.010	0.419	<0.010	
<b>SVM-Moderate vs. others</b>	10.550	<0.005	0.455	<0.010	0.427	<0.010	
<b>SVM-Most Extreme vs. others</b>	5.543	<0.005	0.727	<0.010	0.316	<0.010	
<b>SVM-Normal vs. others</b>	5.274	<0.005	0.827	<0.010	0.261	<0.010	
<b>SVM-Severe vs. others</b>	5.544	<0.005	0.597	<0.010	0.466	<0.010	
<b>SVM-Severe moderate_vs._others</b>	2.131	<0.005	0.662	<0.010	0.462	<0.010	
<b>SVM-Wet vs. Others</b>	1.108	<0.005	0.935	<0.05	0.236	<0.010	

404 Based on Winexpo and SVM model simulation the hazard prone zones have been estimated  
405 (Figure 6). The southern and south-western blocks are extreme drought-prone and northern  
406 and north-western blocks are mild to normal mode. The whole regimes form the coherent  
407 clusters in space highlighted in figure 7. Most extreme to severe drought categories are  
408 clubbed into negative x, y direction and wet categories are clubbed into positive directions of  
409 x and y. Based on the whole aspects of meteorological drought the year wise hazard and  
410 cumulative failure functions are developed. The most extreme, extreme, severe, severe  
411 moderate, moderate and mild categories are included in the category of “hazard prone or  
412 failure “whereas normal, extreme normal and wet categories are included in “censored”  
413 category. Winexpo attains the best result so this model has been used here. According to  
414 simulation of drought category using winexpo, almost 84 observations are fallen into  
415 “hazard-prone” category and 51 observations have fallen into the “censored” group. The  
416 distribution of yearly censored and failure categories are compared based on Weibull and  
417 logistic probability fit but logistic probability fit gave us the better association (Correlation  
418 value 0.984 for logistic and 0.678 for Weibull). So, finally the logistic probability fit have  
419 been taken for year-wise estimation of cumulative hazard-proneness. The whole logistic  
420 model seemed to be more or less normal (Figure 8a and 8b) and it had achieved the 3.223  
421 value as the Anderson-Darling test. From the survival function (Figure 8c) fitted based on  
422 logistic probability plot encounters the fact that as the time (year) will progress the drought  
423 proneness will increase and at the year 2100 the vulnerability will be almost intolerable that  
424 will lead to massive disruption over the local community. Reversely, the progression of  
425 hazard based on cumulative curve plotting (Figure 9, figure 8d) exhibits the fact that the  
426 whole district will be severely affected by drought within 2100. The significance test for  
427 hazard function is done in 95% significance level .So, it can be concluded that the district will  
428 face extreme to severe drought hazard in the recent future.

429

430

431

432

433

434

435

436

437

438

439

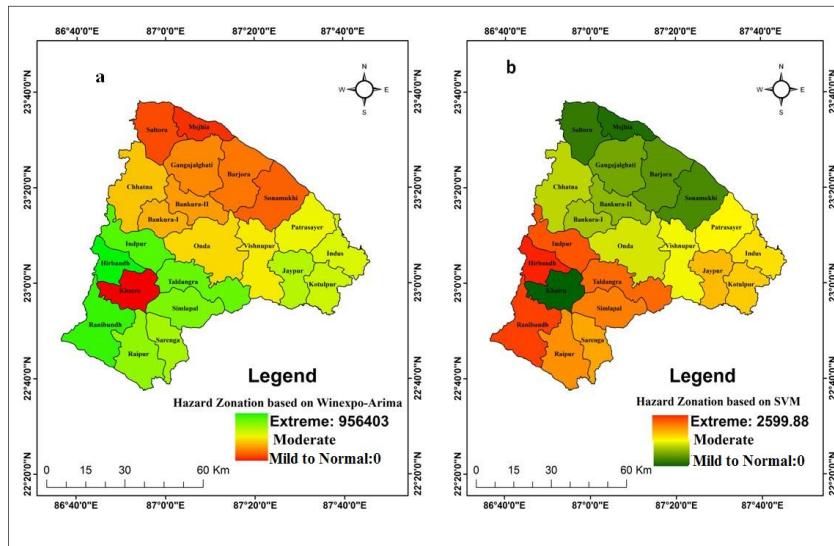
440

441

442

443

444



445 **Figure 6** Drought-prone zone identification (12 month time steps) using a) Winexpo b) SVM

446

447

448

449

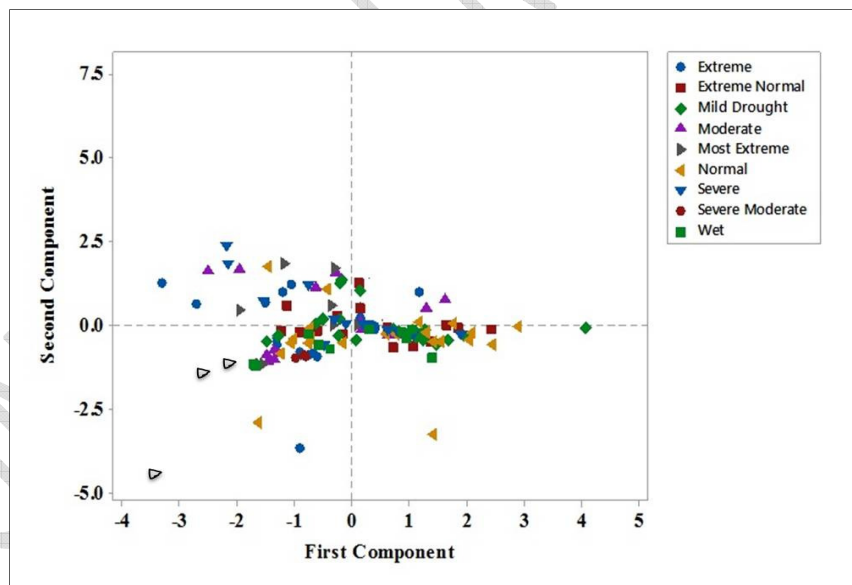
450

451

452

453

454



455 **Figure 7** Plotting of points in the coherent space

456

457

458

459

460

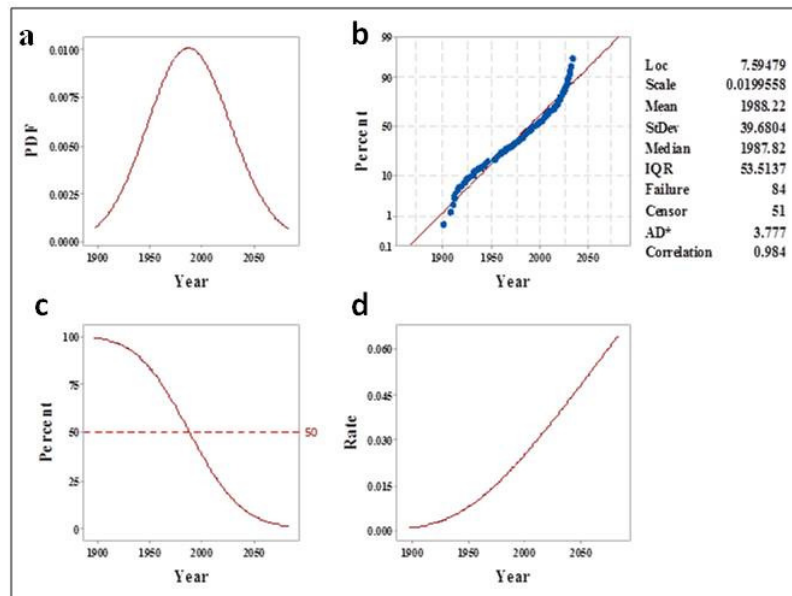
461

462

463

464

465



466 **Figure 8a** Probability density function **b** Logistic probability fit **c** Survival function based on  
 467 logistic probability fit **d** Progression of hazard rate with years

## 468 5. Conclusion

469 The evolution and quantification of drought are necessary for the proper planning and  
 470 management of water resources to mitigate the hazard of future occurrences. By far the main  
 471 challenge in this field is that a) to identify the correct method to analyze the meteorological  
 472 drought b) to identify the spatial dimension over which the drought can be affected c) to  
 473 simulate and predict the drought correctly as it is inherently needed for proper planning and  
 474 management of water resources. Continuous year wise monitoring and simulation is also an  
 475 important issue even seriously neglected in the drought monitoring and assessment. In most  
 476 of the cases of drought monitoring and assessment historical rainfall data is one of the input  
 477 factors. Our study is also not an exception with the above scenarios. Taking rainfall as the  
 478 sole input factor we estimated 6 essential meteorological indices and from those indices we  
 479 form a new index Standardized Total Drought ( $S_d$ ) and simulate it up to 2035 and make a  
 480 comparative assessment of exponential smoothing and machine learning procedures.  
 481 Cumulative drought-proneness of the region using hazard function has been analysed and we  
 482 found that the whole region will be severely drought affected within 2100. The extremities of  
 483 rainfall and temperature drive a potential threat to agriculture, food security and socio-  
 484 economic vulnerability. Thus a more detailed structural study is required to explore the  
 485 synergetic effects of trends and patterns of other climatic variables. However the conclusion

486 reached in this study can be an elementary step to improve the risk management strategy,  
487 review of agricultural practices and water use in this counterpart.

#### 488 **Conflict of Interest**

489 There is no conflict of interest regarding the publication of this article.

#### 490 **References**

- 491 1. Wu Z.Y., Lu G.H., Wen L., Lin C.A. (2011). Reconstructing and Analyzing China's fifty-  
492 nine Year (1951–2009) Drought History using Hydrological Model Simulation. *Hydrol.*  
493 *Earth. Syst. Sci.* 15. 2881-2894. doi: 10.5194/hess-15-2881-2894. URL: [https://www.hydrol-](https://www.hydrol-earth-syst-sci.net/15/2881/2011/)  
494 [earth-syst-sci.net/15/2881/2011/](https://www.hydrol-earth-syst-sci.net/15/2881/2011/)
- 495 2. Zarch A., Amin M.(2015), Droughts In A Warming Climate: A Global Assessment Of  
496 Standardized Precipitation Index (SPI) and Reconnaissance Drought Index (RDI). *J. Hydrol.* .  
497 526. 183-195. URL: <https://www.sciencedirect.com/science/article/pii/S002216941400763X>
- 498 3. Keyantash, J., Dracup, J.A., (2002). The Quantification of Drought: An Evaluation of  
499 Drought Indices. *Bull. Am. Meteorol. Soc.* 83, 1167–1180. URL:  
500 <https://journals.ametsoc.org/doi/abs/10.1175/1520-0477-83.8.1167>.
- 501 4. Lana, X., Burgueno, A.(2000). Statistical Distribution and Spectral Analysis of Rainfall  
502 Anomalies for Barcelona (NE Spain). *Theor. Appl. Climatol.* 66, 211–227. URL:  
503 <https://link.springer.com/article/10.1007/s007040070026>
- 504 5. Dogan, S., Berkday, A., & Singh, V. P. (2012). Comparison of Multi-Monthly Rainfall-  
505 Based Drought Severity Indices, With Application to Semi-Arid Konya Closed Basin,  
506 Turkey. *J. Hydrol.*, 470-471, 255–268. doi:10.1016/j.jhydrol.2012.09.003. URL:  
507 <https://www.sciencedirect.com/science/article/pii/S0022169412007512>.
- 508 6. Wilhite, D. (Ed.), (2000). *Drought: A Global Assessment, vols. I &II. Routledge Hazards*  
509 *and Disasters Series*, Routledge, London. URL:  
510 [https://books.google.co.in/books/about/Drought.html?id=rcNmcgAACAAJ&redir\\_esc=y](https://books.google.co.in/books/about/Drought.html?id=rcNmcgAACAAJ&redir_esc=y).
- 511 7. Duan, K., Xiao, W., Mei, Y., & Liu, D. (2014). Multi-Scale Analysis Of Meteorological  
512 Drought Risks Based on A Bayesian Interpolation Approach In Huai River Basin, China.  
513 *Stoch. Environ. Res. Risk A.*, 28(8), 1985–1998. doi:10.1007/s00477-014-0877-4. URL:  
514 <https://link.springer.com/article/10.1007/s00477-014-0877-4>
- 515 8. Mishra, A.K., Singh, V.P. (2010).A Review of Drought Concepts. *J. Hydrol.* 391, 202-216.  
516 URL: <https://www.sciencedirect.com/science/article/pii/S0022169410004257>

- 517 9. Moghaddasi R., Eghbali A., Rizi P.L. (2014). Analysis and Forecasting of Drought by  
518 Developing a Fuzzy-Based Hybrid Index in Iran. *MPRA*. 1-15. URL: [https://mpra.ub.uni-](https://mpra.ub.uni-muenchen.de/53153/)  
519 [muenchen.de/53153/](https://mpra.ub.uni-muenchen.de/53153/)
- 520 10. Mpelasoka, F., Hennesy, K., Jones, R., Bates, B. (2008). Comparison of Suitable Drought  
521 Indices For Climate Change Impacts Assessment Over Australia Towards Resource  
522 Management. *Int. J. Climatol.* 28, 1283–1292. URL: <http://vuir.vu.edu.au/3851/>
- 523 11. Todisco F., Mannocchi F., Vergni L (2013). Severity Duration-Frequency Curves In the  
524 Mitigation of Drought Impact: An Agricultural Case Study. *Natural Hazards*, 65 (3), 1863.  
525 URL: <https://link.springer.com/article/10.1007/s11069-012-0446-4>
- 526 12. Vicente-Serrano, S.M., Gonzalez-Hidalgo, J.C., De Luis, M., Raventos, J., (2004).  
527 Drought Patterns in the Mediterranean Area: The Valencia Region (Eastern Spain). *Climate*  
528 *Res.* 26, 5–15. URL: <http://digital.csic.es/handle/10261/37069>
- 529 13. Mishra A.K., V. R. Desai, and V. P. Singh, (2007): Drought Forecasting Using a Hybrid  
530 Stochastic and Neural Network Model. *J. Hydrol. Eng.*, 12, 626–638. URL:  
531 [https://ascelibrary.org/doi/abs/10.1061/%28ASCE%2910840699%282007%2912%3A6%286](https://ascelibrary.org/doi/abs/10.1061/%28ASCE%2910840699%282007%2912%3A6%28626%29)  
532 [26%29](https://ascelibrary.org/doi/abs/10.1061/%28ASCE%2910840699%282007%2912%3A6%28626%29)
- 533 14. Abdourahamane, Z. S., & Acar, R. (2018). Fuzzy Rule-Based Forecast of Meteorological  
534 Drought in Western Niger. *Theor Appl Climatol.* doi:10.1007/s00704-017-2365-5.  
535 URL: <https://link.springer.com/article/10.1007/s00704-017-2365-5>
- 536 15. Özger, Mehmet, Ashok K. Mishra, and Vijay P. Singh. (2012). Long Lead Time Drought  
537 Forecasting Using a Wavelet and Fuzzy Logic Combination Model: A Case Study in Texas. *J*  
538 *Hydro. Meteorol.* 13(1): 284–97. <https://doi.org/10.1175/JHM-D-10-05007.1>. URL:  
539 <https://journals.ametsoc.org/doi/full/10.1175/JHM-D-10-05007.1>.
- 540 16. Wilhite, D.A., Hayes, M.J. (1998). Drought planning in the United States: Status and  
541 Future directions. *The Arid Frontier*, Springer, 33-54. URL:  
542 [https://link.springer.com/chapter/10.1007/978-94-011-4888-7\\_2](https://link.springer.com/chapter/10.1007/978-94-011-4888-7_2)
- 543 17. Morid, S., V. Smakhtin, and K. Bagherzadeh, (2007): Drought Forecasting Using  
544 Artificial Neural Networks and Time Series of Drought Indices. *Int. J. Climatol.*, 27, 2103–  
545 2111. URL: <https://rmets.onlinelibrary.wiley.com/doi/10.1002/joc.1498>.
- 546 18. Elhag K.M., Zhang W. (2018). Monitoring and Assessment of Drought Focused on Its  
547 Impact on Sorghum Yield over Sudan by Using Meteorological Drought Indices for the

- 548 Period 2001–2011. *Remote Sens.* 1-21. Doi:10.3390/rs10081231. URL:  
549 <https://www.mdpi.com/2072-4292/10/8/1231>.
- 550 19. Jain S.K., Keshri R., Goswami A., Sarkar A.(2010) Application Of Meteorological And  
551 Vegetation Indices For Evaluation Of Drought Impact: A Case Study For Rajasthan, India.  
552 *Nat. Hazards*, 54 (3), 643. URL: <https://link.springer.com/article/10.1007/s11069-009-9493-x>
- 553 20. Wu, H., Hayes, M.J., Weiss, A., Hu, Q., (2001). An Evaluation of the Standardized  
554 Precipitation Index, the China-Z Index and the Statistical Z-Score. *Int. J. Climatol.* 21, 745–  
555 758. URL: <https://rmets.onlinelibrary.wiley.com/doi/pdf/10.1002/joc.658>
- 556 21. Almedeij, J.(2015). Long-Term Periodic Drought Modeling. *Stochastic Environmental*  
557 *Research and Risk Assessment*, 1-10. URL:[https://link.springer.com/article/10.1007/s00477-](https://link.springer.com/article/10.1007/s00477-015-1065-x)  
558 015-1065-x.
- 559 22. Anderson, M.P.; Woessner, W.W. (1992). *Applied Groundwater Modeling: Simulation of*  
560 *Flow and Advective Transport* (2nd ed.). Academic Press. URL:  
561 [https://www.elsevier.com/books/applied-groundwater-modeling/anderson/978-0-08-091638-](https://www.elsevier.com/books/applied-groundwater-modeling/anderson/978-0-08-091638-5)  
562 5.
- 563 23. Mishra A.K., Desai V.R (2006). Drought Forecasting using Feed-forward Recursive  
564 Neural Network. *Ecol. Model.* pp. 127-138. URL:  
565 <https://www.sciencedirect.com/science/article/pii/S0304380006002055>
- 566 24. Dibike, Y.B., Velickov, S., Solomatine, D., Abbott, M.B., (2001). Model Induction with  
567 Support Vector Machines: Introduction and Applications. *J. Comput. Civil Eng.* 15(3), 208-  
568 216. URL: [https://ascelibrary.org/doi/10.1061/%28ASCE%290887-](https://ascelibrary.org/doi/10.1061/%28ASCE%290887-3801%282001%2915%3A3%28208%29)  
569 3801%282001%2915%3A3%28208%29
- 570 25. Barros, A.P. and G.J. Bowden (2008), Toward Long-Lead Operational Forecasts of  
571 Drought: An Experimental Study in the Murray-Darling River Basin. *J Hydrol.*, 357(3-4):  
572 349-367. URL: <https://www.sciencedirect.com/science/article/pii/S0022169408002540>
- 573 26. Wang, W. C. Men, W. Lu.(2008). Online Prediction Model Based On Support Vector  
574 Machine. *Neurocomputing*, 71: 550-558. URL:  
575 <https://www.sciencedirect.com/science/article/pii/S0925231207002883>.
- 576 27. Wang F.Q., Zheng Z., Kang P.P., Wang L. (2016). Applicability Evaluation On The  
577 Indexes Of Typical Drought In Henan Province, China. *Applied Ecology and Environmental*  
578 *Research*. 253-262. URL: [http://www.aloki.hu/pdf/1503\\_253262.pdf](http://www.aloki.hu/pdf/1503_253262.pdf)



- 579 28. Belayneh A., Adamowski J. (2013). Drought Forecasting Using New Machine Learning  
580 Methods. *Journal of Water and Land Development*.3-12. URL:  
581 <https://content.sciendo.com/view/journals/jwld/18/9/article-p3.xml>
- 582 29. Chatterjee U (2018). Water Scarcity in Semi-Arid Regions of Bankura District, West  
583 Bengal, India – Problems and Prospects. *Khoj*. 87-96. URL:  
584 [https://www.researchgate.net/profile/Uday\\_Chatterjee4/publication/](https://www.researchgate.net/profile/Uday_Chatterjee4/publication/)
- 585 30. Nag S.K, Ghosh P. (2013a). Delineation of Groundwater Potential Zone in Chhatna  
586 Block, Bankura District, West Bengal, India Using Remote Sensing And GIS Techniques.  
587 *Environmental Earth Sciences*. 70(5). 2115-2127. URL:  
588 <https://link.springer.com/article/10.1007/s12665-012-1713-0>
- 589 31. Disaster Management Plan of Bankura District, (2017). Disaster Management Cell. 1-  
590 147. Available at [http://www.wbdmd.gov.in/writereaddata/uploaded/DP/Disaster%](http://www.wbdmd.gov.in/writereaddata/uploaded/DP/Disaster%20Management%20Plan%20of%20Bankura.pdf)  
591 [20Management%20Plan%20of%20Bankura.pdf](http://www.wbdmd.gov.in/writereaddata/uploaded/DP/Disaster%20Management%20Plan%20of%20Bankura.pdf).
- 592 32. Nag S.K, Ghosh P. (2013b). Variation in Groundwater Levels and Water Quality in  
593 Chhatna Block, Bankura District, West Bengal — A GIS Approach. *Journal of Geological*  
594 *Society of India*.81 (2). 261-280. URL: [https://link.springer.com/article/10.1007/s12594-013-](https://link.springer.com/article/10.1007/s12594-013-0029-3)  
595 [0029-3](https://link.springer.com/article/10.1007/s12594-013-0029-3)
- 596 33. Khan J.H., Hassan T. and Shamsad (2011). Socio Economic causes of Rural Urban  
597 Migration in India. *Asia-Pacific Journal of Social Sciences*. 138-158. URL:  
598 <https://www.researchgate.net/publication>
- 599 34. Rogaly B, Biswas J, Coppard D, Rafique A, Rana K and Sengupta (2001) Seasonal  
600 Migration, Social Change and Migrants' Rights: Lessons from West Bengal . *Economic and*  
601 *Political Weekly*. 36(49), 8-14, 4547-4559. URL: <http://sro.sussex.ac.uk/id/eprint/11116/>
- 602 35. Rogaly, B. (2010). Workers on the move: Seasonal Migration and Changing Social  
603 Relations in Rural India. *Gender & Development*, 6(1), 21–29. doi:10.1080/741922628.  
604 URL: <https://www.ncbi.nlm.nih.gov/pubmed/12321533>
- 605 36. District Statistical Handbook, 2014. Collected from Panchayet Bhawan, Salt-Lake city,  
606 Kolkata.

- 607 37. Edwards, D.C., McKee, T.B., 1997. Characteristics of 20th Century Drought in the  
608 United States at Multiple Time Scales. *Atmos. Sci. Paper* .634, 1–30. URL:  
609 <https://mountainscholar.org/handle/10217/170176>.
- 610 38. McKee, T.B., Doesken, N.J., Kleist, J (1993). The Relationship of Drought Frequency  
611 and Duration to Time Scales. *Proceedings of the 8th Conference on Applied Climatology*,  
612 American Meteorological Society Boston, MA , 179-183. URL:  
613 [http://www.droughtmanagement.info/literature/AMS\\_Relationship\\_Drought\\_Frequency\\_Dur](http://www.droughtmanagement.info/literature/AMS_Relationship_Drought_Frequency_Duration_Time_Scales_1993.pdf)  
614 [ation\\_Time\\_Scales\\_1993.pdf](http://www.droughtmanagement.info/literature/AMS_Relationship_Drought_Frequency_Duration_Time_Scales_1993.pdf).
- 615 39. Gibbs, W.J., Maher, J.V. (1967). Rainfall Deciles as Drought Indicators. *Bureau of*  
616 *Meteorology, Bulletin No. 48, Melbourne, Australia.* URL:  
617 <https://trove.nla.gov.au/work/21297477?selectedversion=NBD125659>.
- 618 40. Hayes, M.J., (2006). *Drought Indices*. Van Nostrand's Scientific Encyclopedia, John  
619 Wiley & Sons, Inc. DOI: 10.1002/0471743984.vse859. URL:  
620 <https://onlinelibrary.wiley.com/doi/abs/10.1002/0471743984.vse8593>
- 621 41. Rooy M.P, Van (1965). A Rainfall Anomaly Index Independent of Time and Space.  
622 *Notos*.;14-43p. URL:  
623 <https://www.researchgate.net/deref/http%3A%2F%2Fwww.sid.ir%2Fen%2FVEWSSID%2Fs>  
624 [\\_pdf%2F123E20090104.pdf](https://www.researchgate.net/deref/http%3A%2F%2Fwww.sid.ir%2Fen%2FVEWSSID%2Fs_pdf%2F123E20090104.pdf)
- 625 42. Freitas Mas (2005). Um Sistema De Suporte À Decisão Para O Monitoramento De Secas  
626 Meteorológicas Em Regiões Semiáridas. *Rev. Tecnol.* ; 19: 84-95. URL:  
627 <https://periodicos.unifor.br/tec/article/view/1175>
- 628 43. Chen, S.T., Kuo, C.C., Yu, P.S., (2009). Historical Trends and Variability of  
629 Meteorological Droughts in Taiwan. *Hydrol. Sci. J.* 54 (3), 430–441. URL:  
630 <https://www.tandfonline.com/doi/abs/10.1623/hysj.54.3.430>
- 631 44. <https://otexts.org/fpp2/holt-winters.html>.
- 632 45. Kalekar PS (2004). Time-Series Forecasting Using Holt-Winters Exponential Smoothing.  
633 *Kanwal Rekhi School of Information Technology.* 1-13. Available at:  
634 <https://labs.omniti.com/people/jesus/papers/holtwinters.pdf>.
- 635 46. Vapnik, V.N., Vapnik, V. (1998). *Statistical Learning Theory*. Wiley New York. URL:  
636 <http://www.dsi.unive.it/~pelillo/Didattica/Artificial%20Intelligence/Old%20Stuff/Slides/SLT>  
637 [.pdf](http://www.dsi.unive.it/~pelillo/Didattica/Artificial%20Intelligence/Old%20Stuff/Slides/SLT.pdf)

- 638 47. Vapnik, V. N., Cortes, C., 1995. Support Vector Networks. *Machine Learning* 20, 273–  
639 297. URL: <https://link.springer.com/article/10.1023/A:1022627411411>
- 640 48. Suykens, J.A.K., Lukas, L., Van Dooren, P., De Moor, B., Vandewalle (1999), J. Least  
641 Squares Support Vector Machine Classifiers: A Large Scale Algorithm. *European*  
642 *Conference on Circuit Theory and Design, ECCTD*, Citeseer , 839-842. URL:  
643 <https://perso.uclouvain.be/paul.vandooren/publications/SuykensLVDV99.pdf>.
- 644 49. Suykens, J.A.K., Vandewalle, J.(1999).Least squares support vector machine classifiers  
645 *Neural processing letters* 9, 293-300. URL:  
646 <https://link.springer.com/article/10.1023/A:1018628609742>
- 647 50. Hyndman, Rob J., & Koehler Anne. B. (2006). Another Look at Measures of Forecast  
648 Accuracy. *Int. J. Forecast.* 22 (4). 679-688. URL: <https://robjhyndman.com/papers/mase.pdf>.
- 649 51. Makridakis, Spyros (1993). Accuracy Measures: Theoretical and Practical Concerns. *Int.*  
650 *J. Forecast.* 9 (4): 527-529. URL:  
651 <https://www.sciencedirect.com/science/article/pii/0169207093900793>
- 652 52. Andrews, J. L. and P. D. McNicholas (2011). Mixtures of Modified T-Factor Analyzers  
653 for Model-Based Clustering, Classification, and Discriminant Analysis. *Journal of Statistical*  
654 *Planning and Inference* 141(4), 1479–1486. URL:  
655 <https://www.sciencedirect.com/science/article/pii/S0378375810004830>
- 656 53. Kolmogorov A. (1933). Sulla Determinazione Empirica Di Una Legge Di Distribuzione.  
657 *G. Ist. Ital. Attuari.* 4: 83–91. URL: <http://www.sciepub.com/reference/1552>
- 658 54. Smirnov N (1948). Table for Estimating the Goodness Of Fit Of Empirical Distributions.  
659 *Annals of Mathematical Statistics.* 19: 279– 281. doi:10.1214/aoms/1177730256. URL:  
660 <https://projecteuclid.org/euclid.aoms/1177730256>

661